Physics Letters B 824 (2022) 136802

Contents lists available at ScienceDirect

Physics Letters B

www.elsevier.com/locate/physletb

Next-to-leading order QCD corrections to diphoton-plus-jet production through gluon fusion at the LHC

Simon Badger [a], Thomas Gehrmann [b], Matteo Marcoli [b,*], Ryan Moodie [c]

[a] Dipartimento di Fisica and Arnold-Regge Center, Università di Torino, and INFN, Sezione di Torino, Via P. Giuria 1, 10124 Torino, Italy
[b] Physik-Institut, Universität Zürich, Winthertherstrasse 190, CH-8057 Zürich, Switzerland
[c] Institute for Particle Physics Phenomenology, Department of Physics, Durham University, South Road, Durham, DH1 3LE, UK

ARTICLE INFO

Article history:
Received 24 September 2021
Received in revised form 15 November 2021
Accepted 25 November 2021
Available online 29 November 2021
Editor: B. Grinstein

Keywords:
NLO corrections

ABSTRACT

We compute the next-to-leading order (NLO) QCD corrections to the gluon-fusion subprocess of diphoton-plus-jet production at the LHC. We compute fully differential distributions by combining two-loop virtual corrections with one-loop real radiation using antenna subtraction to cancel infrared divergences. We observe significant corrections at NLO which demonstrate the importance of combining these corrections with the quark-induced diphoton-plus-jet channel at next-to-next-to-leading order (NNLO).

1. Introduction

Recent breakthroughs in two-loop amplitude technology are opening up a new range of precision two-to-three scattering problems. Diphoton-plus-jet production has been one of the first predictions to appear at NNLO in QCD [1]. This progress is extremely timely given the continually improving experimental measurements of diphoton signatures [2]. Predictions for pure diphoton production have been known to NNLO accuracy for some time [3–7]. A q_T-resummed calculation at order $\mathrm{N^3LL'}$ + NNLO was presented recently [8]. Steps towards $\mathrm{N^3LO}$ are being taken with the completion of the three-loop amplitudes [9]. Diphoton-plus-jet signatures are of particular importance at the LHC since they form the largest background to Higgs production at high transverse momenta. The extra jet is necessary to ensure a non-zero transverse momenta in the diphoton system.

The recently computed NNLO corrections [1] of diphoton-plus-jet production display a good perturbative convergence, except in regions where the loop-mediated gluon-fusion process (which contributes to the cross section only from NNLO onwards) is numerically sizable compared to other contributions. In order to capture the full effects of the QCD corrections, it is important to include loop-induced gluon-fusion channels from at least one order higher in the perturbative series. These corrections are the subject of this article.

High precision two-to-three scattering problems have presented an enormous challenge to the theoretical community. The development of new techniques and methodology have been necessary to address several major bottlenecks that have prevented predictions at NNLO in QCD from being completed.

One important ingredient is the two-loop amplitudes for which complete sets of helicity amplitudes have recently been completed [10–13]. These new results have been achieved thanks to a complete understanding of the special functions basis [14–17] and a new range of reduction tools based in finite field arithmetic [18–20]. The end products are fully analytic formulae which can be evaluated efficiently over the phenomenologically relevant phase-space [10–13,21–23].

Combining and integrating the amplitudes into differential cross sections requires the subtraction of infrared divergences. To achieve this in a stable and efficient way is an extremely hard problem and many solutions have been proposed and applied in calculations up to NNLO. Such algorithms often scale poorly with the number of external particles and only a handful of examples for high multiplicity processes at NNLO currently exist [1,24–26].

* Corresponding author.
E-mail addresses: simondavid.badger@unito.it (S. Badger), thomas.gehrmann@uzh.ch (T. Gehrmann), mmarcoli@physik.uzh.ch (M. Marcoli), ryan.i.moodie@durham.ac.uk (R. Moodie).

https://doi.org/10.1016/j.physletb.2021.136802

For the process considered in this article, the infrared divergences are only at NLO. However, since the real radiation involves $2 \to 4$ one-loop squared amplitudes, the automated numerical algorithms are tested in extreme phase-space regions. The leading order (LO) QCD contributions to the gluonic subprocess were first considered in Ref. [27] based on the compact one-loop five-gluon amplitudes [28].

Our paper is organised as follows. We first review the computational setup, discussing the amplitude-level ingredients and antenna subtraction method used to cancel infrared divergences. We then present results for the NLO corrections to differential cross sections at the 13 TeV LHC. We study the perturbative convergence in both transverse momentum and mass variables as well angular distributions in rapidity and the Collins-Soper angle before drawing our conclusions.

2. Computational setup

We consider the scattering process

$$gg \to \gamma\gamma g + X \tag{1}$$

at a hadron collider. As the process is loop-induced, the LO contribution is at order α_s^3 and involves the integration of a one-loop amplitude squared. The NLO QCD corrections are computed by combining the two-loop virtual corrections to the $2 \to 3$ process with the $2 \to 4$ processes with an additional unresolved parton: $gg \to \gamma\gamma gg$ and $gg \to \gamma\gamma q\bar{q}$. Pictorially, we can represent the parton level cross sections up to NLO in QCD as,

$\sigma^{\text{NLO}}_{gg\to\gamma\gamma g+X} =$ 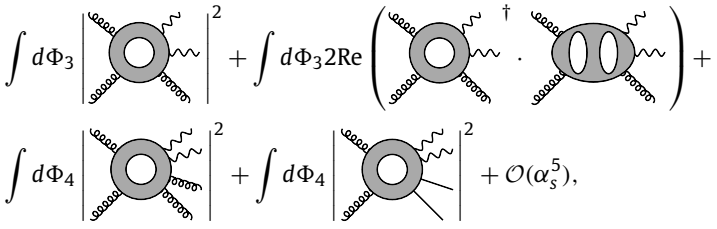

$+ \mathcal{O}(\alpha_s^5),$ (2)

where $d\Phi_n$ represents the on-shell phase-space measure for n massless final state particles. The one-loop amplitude for $q\bar{q}gg\gamma\gamma$ indicates the loop contribution in which the photons couple to an internal fermion loop. The observable process $pp \to \gamma\gamma j$ also includes channels where the photons couple to an external quark pair. The expansion up to the NNLO of $pp \to \gamma\gamma j$ includes terms up to $\mathcal{O}(\alpha_s^3)$ and so the contributions coming from Eq. (2) are technically N^{3}LO. However, due to the large gluon flux at high energy hadron colliders, such contributions can be significant.

The one-loop amplitudes for the LO process and the real correction are finite, since the corresponding tree-level processes vanish. The renormalised two-loop five-particle amplitude contains explicit infrared divergences generated by the integration over the loop momenta, while the one-loop six-particle amplitudes exhibit a divergent behavior when a final-state parton becomes unresolved. The divergences cancel in the final result, as established by the KLN theorem, and a finite remainder of the virtual amplitudes can be defined using QCD factorization [29]. In our calculation, this cancellation is performed using the antenna subtraction method [30–32]. The method extracts the infrared singular contributions from the real radiation subprocess, and combines their integrated form with the virtual subprocess, thus enabling their numerical integration using Monte Carlo methods, performed here in the NNLOJET framework. The QCD structure of the process under consideration is very similar to Higgs-plus-jet production in gluon fusion, which has been computed previously [33,34] using antenna subtraction, and identical antenna subtraction terms are applied here.

The infrared-finite remainders of the two-loop amplitudes have recently been computed [13] using a basis of pentagon functions [14,15,17], which permit efficient and reliable numerical evaluation [17]. The full colour and helicity summed expressions are obtained from the NJET amplitude library. Within NJET, a dimension scaling test is performed for each phase-space point to assess the accuracy of the evaluation. If the test is unsuccessful, the point is recomputed in higher precision. We set a three digits accuracy threshold for this test, which guarantees a stable result without significantly affecting the performance.

The one-loop six-particle amplitudes are obtained using a combination of implementations from the OPENLOOPS2 [35] generator and from the generalised unitarity [36–38] approach within NJET [39]. We use an improved version of OPENLOOPS2 in combination with the new extension OTTER. OTTER [40] is a tensor integral library based on the *on-the-fly reduction* [41] of OPENLOOPS2 and on stability improvements described in Ref. [35]. This new version of OPENLOOPS2 allows for a stable computation of the needed one-loop squared amplitudes in deep infrared regions. Internally, OTTER uses double-precision scalar integrals that are provided by COLLIER [42,43], as well as quad-precision scalar integrals provided by ONELOOP [44]. Minor modifications were made in NJET to avoid de-symmetrisation over the two photons and allow for a pointwise correspondence with the subtraction terms. To compute the one-loop amplitude $gggg\gamma\gamma$, the OPENLOOPS implementation was generally more efficient, but for exceptional phase-space points it was necessary to use the high precision (32 digits) implementation within NJET. For the $q\bar{q}gg\gamma\gamma$ channel, we used NJET, which allowed for a straightforward selection of the required loop contribution. We note that this amplitude is also available within OPENLOOPS2 and we checked that the two implementations agree.

The amplitude-level ingredients have been validated in all relevant collinear and soft limits by checking their convergence towards the respective antenna subtraction terms.

3. Results

For the numerical evaluation of our NLO results on the gluon-induced diphoton-plus-jet process, we apply the same kinematical cuts as were used for the NNLO calculation [1] of the quark-induced processes. These represent a realistic setup relevant for physics studies at the 13 TeV LHC. The cuts are as follows:

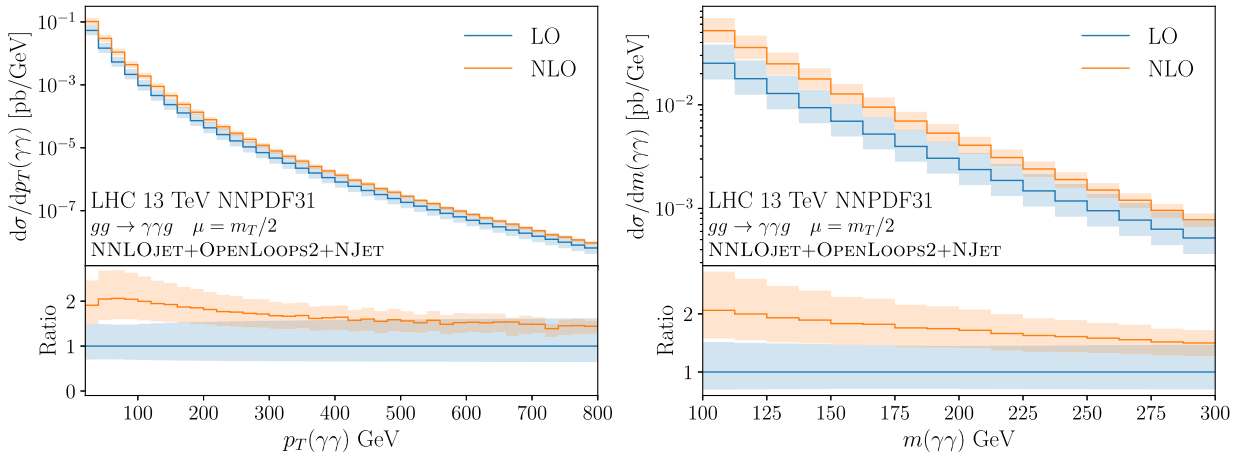

Fig. 1. Differential distributions in the transverse momentum $p_T(\gamma\gamma)$ (left) and invariant mass $m(\gamma\gamma)$ (right) of the diphoton system.

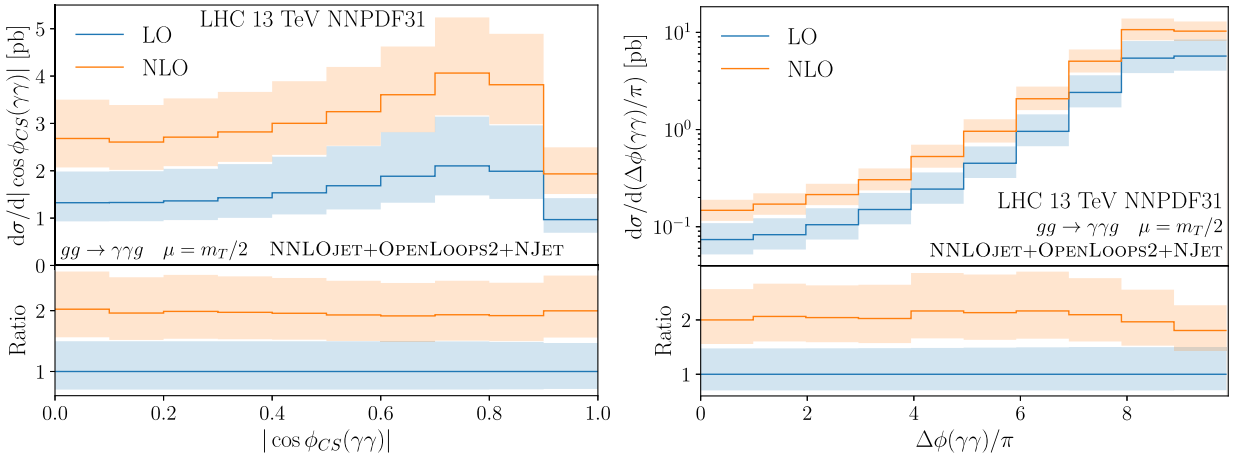

Fig. 2. Differential distributions in the Collins-Soper angle $|\cos\phi_{CS}(\gamma\gamma)|$ (left) the azimuthal decorrelation $\Delta\phi(\gamma\gamma)$ (right) of the diphoton system.

- minimum photon transverse momenta and rapidities: $p_T(\gamma_1) > 30$ GeV, $p_T(\gamma_2) > 18$ GeV and $|\eta(\gamma\gamma)| < 2.4$.
- smooth photon isolation criterion [45] with $\Delta R_0 = 0.4$, $E_T^{\max} = 10$ GeV and $\epsilon = 1$.
- minimal invariant mass of the photon pair: $m(\gamma\gamma) \geq 90$ GeV.
- minimal separation of the photons: $\Delta R_{\gamma\gamma} > 0.4$.
- minimal transverse momentum of the photon pair: $p_T(\gamma\gamma) > 20$ GeV.

We consider kinematical distributions in the following diphoton variables: transverse momentum of the diphoton system $p_T(\gamma\gamma)$, pair invariant mass $m_{\gamma\gamma}$, diphoton total rapidity $|y(\gamma\gamma)|$ and rapidity difference $\Delta y(\gamma\gamma)$, as well as Collins-Soper angle $|\phi_{CS}(\gamma\gamma)|$ [46] and azimuthal decorrelation $\Delta\phi(\gamma\gamma)$. For these distributions, no jet requirement is applied, as done in Ref. [1], since the transverse momentum cut on the diphoton system is already sufficient to avoid NNLO-like configurations where all final-state QCD partons become unresolved.

Our numerical results use the NNLO set of the NNPDF3.1 parton distribution functions [47] throughout, thus allowing a straightforward comparison with the existing NNLO results [1] in the quark-initiated channels. The strong coupling constant is evaluated using LHAPDF [48], with $\alpha_s(m_Z) = 0.118$. The electromagnetic coupling constant is set to $\alpha = 1/137.035999139$. Monte Carlo integration errors are below 1% on average and not displayed in the plots.

The uncertainty on our theory predictions is estimated by a seven-point variation of the renormalisation and factorisation scales around a central value, chosen in dynamical manner on event-by-event basis to be

$$\mu_F = \mu_R = \frac{1}{2} m_T = \frac{1}{2} \left(m^2(\gamma\gamma) + p_T^2(\gamma\gamma) \right)^{1/2} \tag{3}$$

Figs. 1–3 display the theory predictions for the different single-differential distributions in the diphoton variables. We observe the NLO corrections to be very sizable, often being comparable in size to the LO predictions. The corrections are largest at low $p_T(\gamma\gamma)$ or at low invariant mass, Fig. 1, where the NLO/LO ratio reaches 2 and NLO and LO uncertainties fail to overlap, while the ratio is smoothly decreasing towards values of 1.5 for large $p_T(\gamma\gamma)$ or $m(\gamma\gamma)$, with overlapping scale uncertainty bands above $p_T(\gamma\gamma) = 200$ GeV or $m(\gamma\gamma) = 175$ GeV.

The integrated cross section is dominated by the region of low $p_T(\gamma\gamma)$ or low $m(\gamma\gamma)$, such that distributions that are differential only in geometrical photon variables, Figs. 2 and 3, display typically near-uniform NLO/LO ratios of 2, and no overlap of the LO and NLO scale uncertainty bands. Visually, the scale uncertainty bands at NLO and LO appear to be of comparable width in all distributions. However, owing to the large size of the NLO corrections, the relative scale uncertainty is reduced from about 50% at LO to 30% at NLO.

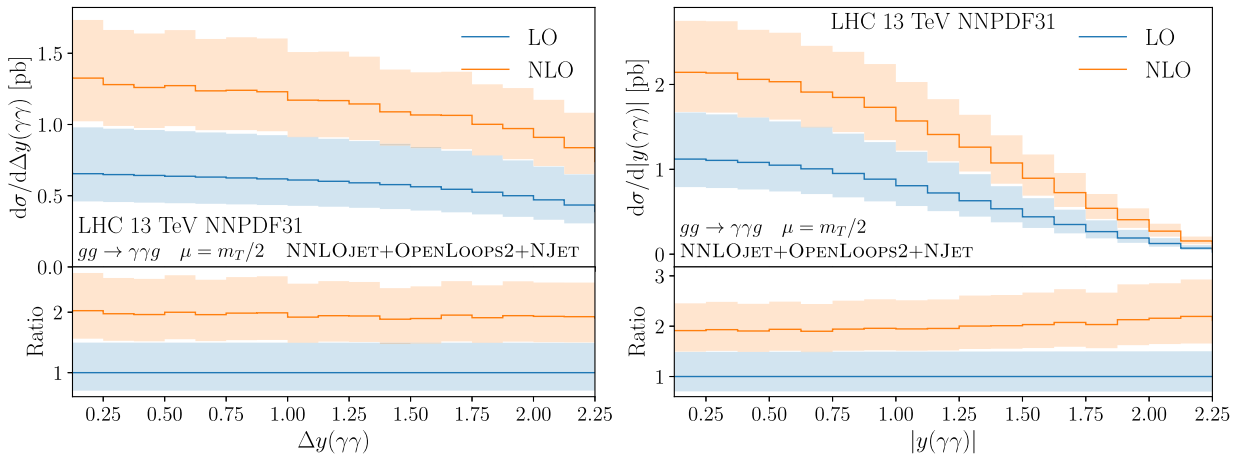

Fig. 3. Differential distributions in the diphoton rapidity difference $\Delta y(\gamma\gamma)$ (left) and the diphoton total rapidity $|y(\gamma\gamma)|$ (right).

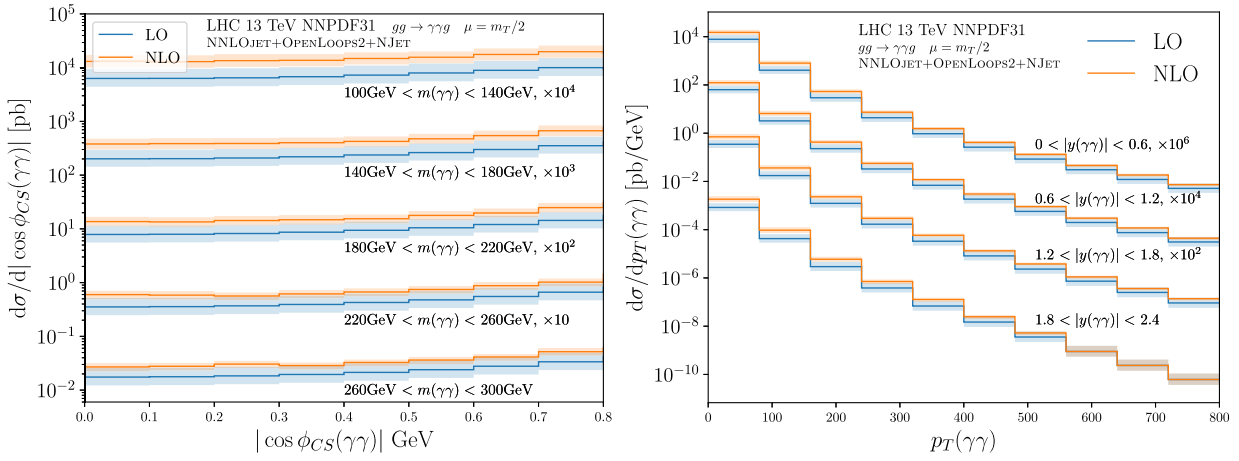

Fig. 4. Two-dimensional differential distributions in the diphoton invariant mass $m(\gamma\gamma)$ and Collins-Soper angle $|\phi_{CS}(\gamma\gamma)|$ (left) and in the diphoton rapidity $|y(\gamma\gamma)|$ and transverse momentum $p_T(\gamma\gamma)$ (right).

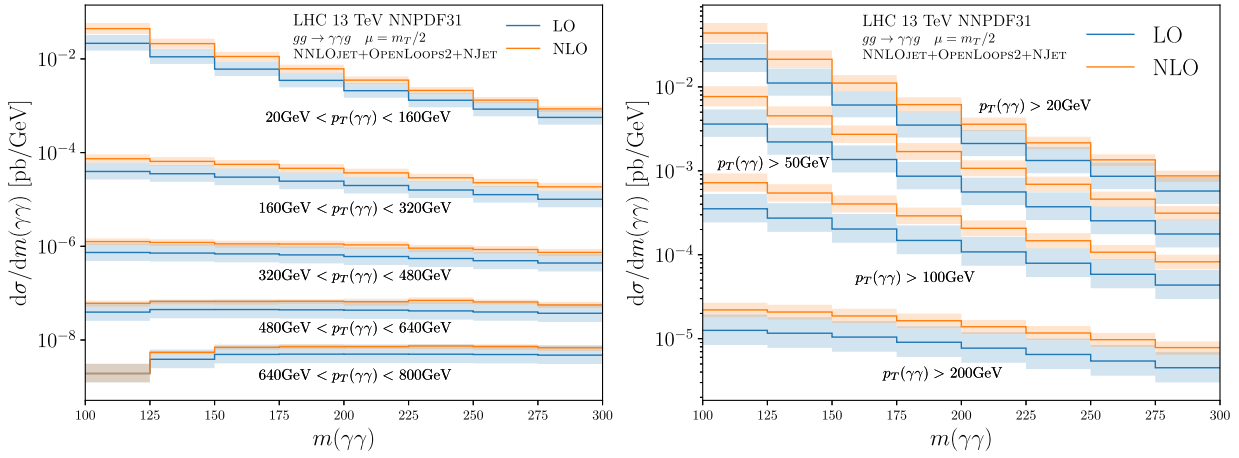

Fig. 5. Two-dimensional differential distributions in the diphoton transverse momentum $p_T(\gamma\gamma)$ and invariant mass $m(\gamma\gamma)$, in bins in $p_T(\gamma\gamma)$ (left) and for varying lower $p_T(\gamma\gamma)$-cut (right).

By inspecting the two-dimensional differential distribution in $m(\gamma\gamma)$ and $|\phi_{CS}(\gamma\gamma)|$, Fig. 4 (left), we observe that the relative magnitude of the NLO corrections decreases with increasing $m(\gamma\gamma)$, while the corrections remain uniform in $|\phi_{CS}(\gamma\gamma)|$ for all bins in $m(\gamma\gamma)$. The two-dimensional differential distribution in $|y(\gamma\gamma)|$ and $p_T(\gamma\gamma)$ also shows the decrease of the corrections towards larger $p_T(\gamma\gamma)$. The decrease is more pronounced at forward rapidity than at central rapidity.

Considering two-dimensional distributions in $p_T(\gamma\gamma)$ and $m(\gamma\gamma)$, Fig. 5, largely reproduces the features of the one-dimensional distributions of Fig. 1, both for distributions in bins of $p_T(\gamma\gamma)$ or for varying lower cut in $p_T(\gamma\gamma)$. The only novel feature is a non-uniform

shape in $m(\gamma\gamma)$ for the highest bin in $p_T(\gamma\gamma)$ (lowest curves in left Fig. 5), which is indicative of the onset of large logarithmic corrections in $\log(m(\gamma\gamma)/p_T(\gamma\gamma))$ in this range.

The numerical size of the NLO corrections and the scale uncertainties at LO and NLO are comparable to what was observed in inclusive Higgs boson production in gluon fusion [49] or in the Higgs boson transverse momentum distribution in gluon fusion [50,51]. These processes are mediated through a heavy top quark loop and are very similar to the diphoton-plus-jet production considered here in terms of kinematics and initial-state parton momentum range. The pathology of the NLO corrections observed here is thus not that surprising after all; it does however indicate the potential numerical importance of corrections beyond NLO.

The Born-level $gg \to \gamma\gamma g$ subprocess (corresponding to the LO in our results) contributes to the full diphoton-plus-jet production as part of the NNLO corrections. Corrections to this order were computed most recently [1]: these were observed to be moderate and within the scale uncertainty of the previously known NLO results for most of the kinematical range, where they also led to a substantial reduction of the scale uncertainty at NNLO. Only at low $p_T(\gamma\gamma)$ or low $m(\gamma\gamma)$, larger positive corrections and an increased scale uncertainty were observed [1]. These effects could be identified to be entirely due to the contribution of the $gg \to \gamma\gamma g$, which only starts to contribute from NNLO onwards, and it was anticipated in Ref. [1] that NLO corrections to the $gg \to \gamma\gamma g$ (which form a subset of the $\mathrm{N^3LO}$ corrections to the full diphoton-plus-jet process) could help to stabilise the predictions in the relevant kinematical ranges.

Our results demonstrate that this is not the case. The absolute scale uncertainty on the gluon-induced process does not decrease from LO to NLO, and the NLO correction is of about the size of the LO contribution. Consequently, inclusion of the NLO corrections to the $gg \to \gamma\gamma g$ into the full NNLO diphoton-plus-jet process will further enhance the predictions at low $p_T(\gamma\gamma)$ or low $m(\gamma\gamma)$, thereby further elongating them from the previously known order, and will leave the scale uncertainty band largely unchanged.

4. Conclusions

In this article, we have presented the NLO QCD corrections to the diphoton-plus-jet production in the gluon-fusion channel for the first time. The loop-induced process requires the evaluation of six-point one-loop real emission amplitudes and full-colour five-point two-loop virtual amplitudes. To the best of our knowledge it is the first time that five-point two-loop amplitudes with the full colour information have been integrated to provide fully differential cross section predictions relevant for the LHC experiments.

Using a realistic set of kinematic cuts and simulation parameters, we find significant corrections at NLO. This is particularly relevant at low values of $p_T(\gamma\gamma)$ and $m(\gamma\gamma)$. Since angular observables such as rapidity and the Collins-Soper angle are inclusive over the energy variables, one observes significant NLO corrections across the full parameter range. Double differential distributions further highlight this feature, which is reminiscent of the perturbative convergence observed in other gluon-induced processes such as inclusive Higgs production and the Higgs boson transverse momentum distribution. The relative scale uncertainty is reduced by the higher order corrections, although in absolute terms the scale uncertainty does not decrease from LO to NLO in the low $p_T(\gamma\gamma)$ and $m(\gamma\gamma)$ regions.

This work demonstrates the importance of a combined prediction for quark-induced and gluon-induced diphoton-plus-jet signatures for future precision studies at the LHC.

Declaration of competing interest

The authors declare that they have no known competing financial interests or personal relationships that could have appeared to influence the work reported in this paper.

Acknowledgements

We would like to thank Johannes Henn, Xuan Chen, Alexander Huss and Simone Zoia for numerous discussions and interesting input in the course of this project. Help with OpenLoops2 from Jean-Nicolas Lang and Federico Buccioni is gratefully acknowledged. This research has been supported in part by the Swiss National Science Foundation (SNF) under contract number 200020-175595 and by the Swiss National Supercomputing Centre (CSCS) under project ID UZH10. This project received funding from the European Union's Horizon 2020 research and innovation programme *High precision multi-jet dynamics at the LHC* (ERC Consolidator grant agreement No. 772009). RM was supported by STFC grants ST/S505365/1 and ST/P001246/1.

References

[1] H.A. Chawdhry, M. Czakon, A. Mitov, R. Poncelet, NNLO QCD corrections to diphoton production with an additional jet at the LHC, arXiv:2105.06940, 2021.
[2] G. Aad, et al., Measurement of the production cross section of pairs of isolated photons in pp collisions at 13 TeV with the ATLAS detector, arXiv:2107.09330, 2021.
[3] C. Anastasiou, E.W.N. Glover, M.E. Tejeda-Yeomans, Two loop QED and QCD corrections to massless fermion boson scattering, Nucl. Phys. B 629 (2002) 255–289, arXiv:hep-ph/0201274.
[4] Z. Bern, A. De Freitas, L.J. Dixon, Two loop amplitudes for gluon fusion into two photons, J. High Energy Phys. 09 (2001) 037, arXiv:hep-ph/0109078.
[5] S. Catani, L. Cieri, D. de Florian, G. Ferrera, M. Grazzini, Diphoton production at hadron colliders: a fully-differential QCD calculation at NNLO, Phys. Rev. Lett. 108 (2012) 072001, Erratum: Phys. Rev. Lett. 117 (2016) 089901, arXiv:1110.2375.
[6] J.M. Campbell, R.K. Ellis, Y. Li, C. Williams, Predictions for diphoton production at the LHC through NNLO in QCD, J. High Energy Phys. 07 (2016) 148, arXiv:1603.02663.
[7] T. Gehrmann, N. Glover, A. Huss, J. Whitehead, Scale and isolation sensitivity of diphoton distributions at the LHC, J. High Energy Phys. 01 (2021) 108, arXiv:2009.11310.
[8] T. Neumann, The diphoton q_T spectrum at $\mathrm{N^3LL'}$ + NNLO, Eur. Phys. J. C 81 (10) (2021) 905, arXiv:2107.12478.
[9] F. Caola, A. Von Manteuffel, L. Tancredi, Diphoton amplitudes in three-loop quantum chromodynamics, Phys. Rev. Lett. 126 (2021) 112004, arXiv:2011.13946.
[10] B. Agarwal, F. Buccioni, A. von Manteuffel, L. Tancredi, Two-loop leading colour QCD corrections to $q\bar{q} \to \gamma\gamma g$ and $qg \to \gamma\gamma q$, J. High Energy Phys. 04 (2021) 201, arXiv:2102.01820.
[11] H.A. Chawdhry, M. Czakon, A. Mitov, R. Poncelet, Two-loop leading-colour QCD helicity amplitudes for two-photon plus jet production at the LHC, J. High Energy Phys. 07 (2021) 164, arXiv:2103.04319.
[12] B. Agarwal, F. Buccioni, A. von Manteuffel, L. Tancredi, Two-loop helicity amplitudes for diphoton plus jet production in full color, arXiv:2105.04585, 2021.
[13] S. Badger, C. Brønnum-Hansen, D. Chicherin, T. Gehrmann, H.B. Hartanto, J. Henn, M. Marcoli, R. Moodie, T. Peraro, S. Zoia, Virtual QCD corrections to gluon-initiated diphoton plus jet production at hadron colliders, arXiv:2106.08664, 2021.
[14] D. Chicherin, J. Henn, V. Mitev, Bootstrapping pentagon functions, J. High Energy Phys. 05 (2018) 164, arXiv:1712.09610.
[15] T. Gehrmann, J. Henn, N. Lo Presti, Pentagon functions for massless planar scattering amplitudes, J. High Energy Phys. 10 (2018) 103, arXiv:1807.09812.

[16] D. Chicherin, T. Gehrmann, J. Henn, P. Wasser, Y. Zhang, S. Zoia, All master integrals for three-jet production at next-to-next-to-leading order, Phys. Rev. Lett. 123 (2019) 041603, arXiv:1812.11160.
[17] D. Chicherin, V. Sotnikov, Pentagon functions for scattering of five massless particles, J. High Energy Phys. 12 (2020) 167, arXiv:2009.07803.
[18] A. von Manteuffel, R.M. Schabinger, A novel approach to integration by parts reduction, Phys. Lett. B 744 (2015) 101–104, arXiv:1406.4513.
[19] T. Peraro, Scattering amplitudes over finite fields and multivariate functional reconstruction, J. High Energy Phys. 12 (2016) 030, arXiv:1608.01902.
[20] T. Peraro, FiniteFlow: multivariate functional reconstruction using finite fields and dataflow graphs, J. High Energy Phys. 07 (2019) 031, arXiv:1905.08019.
[21] S. Abreu, B. Page, E. Pascual, V. Sotnikov, Leading-color two-loop QCD corrections for three-photon production at hadron colliders, J. High Energy Phys. 01 (2021) 078, arXiv:2010.15834.
[22] H.A. Chawdhry, M. Czakon, A. Mitov, R. Poncelet, Two-loop leading-color helicity amplitudes for three-photon production at the LHC, J. High Energy Phys. 06 (2021) 150, arXiv:2012.13553.
[23] S. Abreu, F.F. Cordero, H. Ita, B. Page, V. Sotnikov, Leading-color two-loop QCD corrections for three-jet production at hadron colliders, J. High Energy Phys. 07 (2021) 095, arXiv:2102.13609.
[24] M. Czakon, A. Mitov, R. Poncelet, Next-to-next-to-leading order study of three-jet production at the LHC, Phys. Rev. Lett. 127 (15) (2021) 152001, arXiv:2106.05331.
[25] H.A. Chawdhry, M.L. Czakon, A. Mitov, R. Poncelet, NNLO QCD corrections to three-photon production at the LHC, J. High Energy Phys. 02 (2020) 057, arXiv:1911.00479.
[26] S. Kallweit, V. Sotnikov, M. Wiesemann, Triphoton production at hadron colliders in NNLO QCD, Phys. Lett. B 812 (2021) 136013, arXiv:2010.04681.
[27] D. de Florian, Z. Kunszt, Two photons plus jet at LHC: the NNLO contribution from the gg initiated process, Phys. Lett. B 460 (1999) 184–188, arXiv:hep-ph/9905283.
[28] Z. Bern, L.J. Dixon, D.A. Kosower, One loop corrections to five gluon amplitudes, Phys. Rev. Lett. 70 (1993) 2677–2680, arXiv:hep-ph/9302280.
[29] S. Catani, The singular behavior of QCD amplitudes at two loop order, Phys. Lett. B 427 (1998) 161–171, arXiv:hep-ph/9802439.
[30] A. Gehrmann-De Ridder, T. Gehrmann, E.W.N. Glover, Antenna subtraction at NNLO, J. High Energy Phys. 09 (2005) 056, arXiv:hep-ph/0505111.
[31] A. Daleo, T. Gehrmann, D. Maitre, Antenna subtraction with hadronic initial states, J. High Energy Phys. 04 (2007) 016, arXiv:hep-ph/0612257.
[32] J. Currie, E.W.N. Glover, S. Wells, Infrared structure at NNLO using antenna subtraction, J. High Energy Phys. 04 (2013) 066, arXiv:1301.4693.
[33] X. Chen, T. Gehrmann, E.W.N. Glover, M. Jaquier, Precise QCD predictions for the production of Higgs + jet final states, Phys. Lett. B 740 (2015) 147–150, arXiv:1408.5325.
[34] X. Chen, J. Cruz-Martinez, T. Gehrmann, E.W.N. Glover, M. Jaquier, NNLO QCD corrections to Higgs boson production at large transverse momentum, J. High Energy Phys. 10 (2016) 066, arXiv:1607.08817.
[35] F. Buccioni, J.-N. Lang, J.M. Lindert, P. Maierhöfer, S. Pozzorini, H. Zhang, M.F. Zoller, OpenLoops 2, Eur. Phys. J. C 79 (2019) 866, arXiv:1907.13071.
[36] Z. Bern, L.J. Dixon, D.C. Dunbar, D.A. Kosower, One loop n point gauge theory amplitudes, unitarity and collinear limits, Nucl. Phys. B 425 (1994) 217–260, arXiv:hep-ph/9403226.
[37] Z. Bern, L.J. Dixon, D.C. Dunbar, D.A. Kosower, Fusing gauge theory tree amplitudes into loop amplitudes, Nucl. Phys. B 435 (1995) 59–101, arXiv:hep-ph/9409265.
[38] R. Britto, F. Cachazo, B. Feng, Generalized unitarity and one-loop amplitudes in N=4 super-Yang-Mills, Nucl. Phys. B 725 (2005) 275–305, arXiv:hep-th/0412103.
[39] S. Badger, B. Biedermann, P. Uwer, V. Yundin, Numerical evaluation of virtual corrections to multi-jet production in massless QCD, Comput. Phys. Commun. 184 (2013) 1981–1998, arXiv:1209.0100.
[40] J.-N. Lang, et al., OTTER: On-The-fly TEnsor Reduction, in press.
[41] F. Buccioni, S. Pozzorini, M. Zoller, On-the-fly reduction of open loops, Eur. Phys. J. C 78 (2018) 70, arXiv:1710.11452.
[42] A. Denner, S. Dittmaier, L. Hofer, COLLIER - a fortran-library for one-loop integrals, PoS LL2014 (2014) 071, arXiv:1407.0087.
[43] A. Denner, S. Dittmaier, L. Hofer, Collier: a fortran-based complex one-loop library in extended regularizations, Comput. Phys. Commun. 212 (2017) 220–238, arXiv:1604.06792.
[44] A. van Hameren, OneLOop: for the evaluation of one-loop scalar functions, Comput. Phys. Commun. 182 (2011) 2427–2438, arXiv:1007.4716.
[45] S. Frixione, Isolated photons in perturbative QCD, Phys. Lett. B 429 (1998) 369–374, arXiv:hep-ph/9801442.
[46] J.C. Collins, D.E. Soper, Angular distribution of dileptons in high-energy hadron collisions, Phys. Rev. D 16 (1977) 2219.
[47] R.D. Ball, et al., Parton distributions from high-precision collider data, Eur. Phys. J. C 77 (2017) 663, arXiv:1706.00428.
[48] A. Buckley, J. Ferrando, S. Lloyd, K. Nordström, B. Page, M. Rüfenacht, M. Schönherr, G. Watt, LHAPDF6: parton density access in the LHC precision era, Eur. Phys. J. C 75 (2015) 132, arXiv:1412.7420.
[49] A. Djouadi, M. Spira, P.M. Zerwas, Production of Higgs bosons in proton colliders: QCD corrections, Phys. Lett. B 264 (1991) 440–446.
[50] D. de Florian, M. Grazzini, Z. Kunszt, Higgs production with large transverse momentum in hadronic collisions at next-to-leading order, Phys. Rev. Lett. 82 (1999) 5209–5212, arXiv:hep-ph/9902483.
[51] V. Ravindran, J. Smith, W.L. Van Neerven, Next-to-leading order QCD corrections to differential distributions of Higgs boson production in hadron–hadron collisions, Nucl. Phys. B 634 (2002) 247–290, arXiv:hep-ph/0201114.